ANALYTICAL APPROACH OF ANCHOR ROD STIFFNESS AND STEEL BASE-PLATE CALCULATION UNDER TENSION

Konstantinos Daniel Tsavdaridis[1*], Mohamed A. Shaheen[2], Charalampos Baniotopoulos[3] and Emad Salem[4]

[1] *Institute for Resilient Infrastructure, School of Civil Engineering, University of Leeds, LS2 9JT, Leeds, UK, k.tsavdaridis@leeds.ac.uk*
[2, 4] *Department of Civil Engineering, Al-Azhar University, Cairo, Egypt*
[3] *School of Civil Engineering, University of Birmingham, B15 2TT, Birmingham, UK*
[*] *Corresponding Author*

ABSTRACT

The analysis of column base plate connections under biaxial moment or when large numbers of anchor rods are utilised is complicated. Such complex connections are regularly found in engineering practice, in spite of proposed, up-to-date finite element modelling techniques and analytical formulations being unsuitable. The lack of suitability arises from their development for non-practical column base plate idealised configurations. In the present paper the results of a finite element study of single-headed anchors under tension are discussed, leading to the derivation of a simple equation that describes the stiffness of the headed anchor rod embedded in concrete. Furthermore, this paper suggests a simple and suitable approach to analyse base plate connections independent of loading scenarios, the number of anchor rods and their arrangement, taking into account the actual rigidity of the connection. In this study, a three-dimensional, nonlinear finite element model is developed through the use of the general-purpose finite element software package ABAQUS. The respective numerical results were verified against experimental ones.

Key words: steel column base; base plate; tension load; monotonic tension load; anchor rod; holding down bolt; parametric study; rod stiffness

1. Introduction

It is well known that the design of base plates is of paramount importance. They are one of the most critical components in steel structures as they control the initial stiffness of the frame depending upon the type and properties of the assemblage. Inevitably, a few components of a column base plate in tension are particularly influential in regards to the stiffness of the connection [1]. Anchor rods are used to transfer the tensile load and/or shear load to the concrete foundation. Anchor rods are divided into two main categories according to the method of construction, namely, cast-in-place anchors and post-installed anchors. Post-installed anchors are placed after the concrete sets. Hence, they are not recommended for base plates; their design is governed by the manufacturer's specifications [6]. According to ACI [2], cast-in-place anchorage systems are the headed rods, the hooked rods (J- or L- rod) and the headed studs, as they are depicted in **Fig. 1**. Among the different types of cast-in-place anchors, the most commonly used in engineering practice is the headed rod/stud. Other types are not very effective in transferring tension forces, particularly in the case of high-strength rods [5]. The paper is limited to study the cast-in-place anchor rod with an anchor plate at the end of the embedment depth (i.e. headed anchor rod).

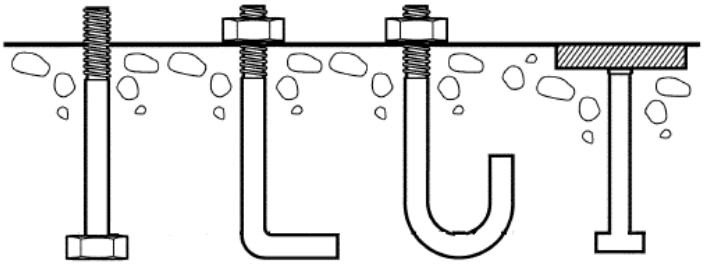

Fig. 1: Types of cast-in-place anchor rods [2]

The mechanism by which the load is transferred from the headed anchor rod to the concrete foundation involves two stages: (i) the bond between the anchor rod and the concrete, and (ii) the bearing on the head of the anchor rod. These two mechanisms do not take place simultaneously. Thus, they can be considered independently [3-[4]. The failure mode of the headed anchor is controlled by various factors including the concrete strength, steel strength, embedment depth, and edge distance. In the case of the headed anchor rod subject to tension forces, five different failure modes typically were observed in past experimental tests [4][[12-[15], as demonstrated in **Fig. 2**. Steel failure occurs through yielding and rapture of the anchor rod. In such a failure mode, the maximum rod capacity is reached. Pullout failure is characterised by the pulling out of the anchor rod from the concrete. This may be followed by the formation of a shallow concrete cone as the head of the anchor approaches the concrete surface. This mode of failure mostly arises when small anchor head diameters are used, in conjunction with expected high-stress concentrations [10-[11]. Concrete breakout failure is very common in engineering practice with anchors experiencing such failure prior to the yielding of the steel. The primary factors affecting this type of failure are the concrete tensile strength, the anchor head diameter, and the embedment depth. Concrete blowout may also control the design, particularly when long anchors are positioned near the free edge of the concrete block.

When the concrete block dimensions are small in relation to the anchors' size, or the free edge distance is small, splitting of the concrete occurs.

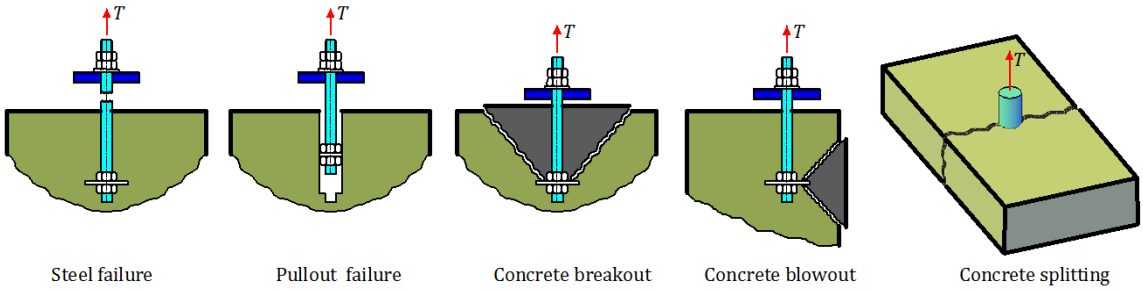

Fig. 2: Failure modes for anchors

The so-called component method is the current state-of-the-art analytical technique to model the steel-concrete composite (SCC) behaviour; decomposes the SCC model into a set of individual basic components. The mechanical properties (e.g. resistance, stiffness and deformation capacity) of each component are then studied individually before being combined to define the mechanical properties of the overall SCC model. The use of the component method in modelling of column bases connections gives an accurate prediction of their behaviour [17]. In this paper, the component method is employed for the study of the base plate connection behaviour considering an anchor rod subjected to tension force

There is a plethora of research in the literature discussing the performance of column base plate connections. Numerous papers propose different analytic, mathematical equations to anticipate the structural behaviour and resistance capacity of column base plate connections [18-[22]. The previously suggested equations are applicable for standard connections with two or four anchor rods. Analysis of column base plate connections under biaxial moments or when large numbers of anchor rods are utilised is complicated. Such complex connections are regularly found in engineering practice, despite their lack of suitability. Proposed, up-to-date finite element (FE) modelling techniques, and proposed analytical formulations are unsuitable due to their development for ideal (and often non-practical) column base plate configurations (**Fig. 3**).

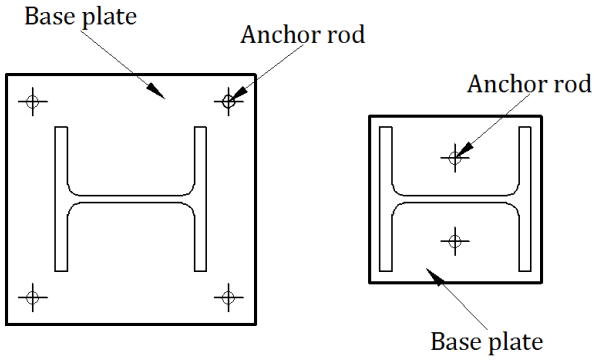

Fig. 3: Standard column bases

Practising engineers use commercial structural software, with suitable reliability and speed to setup a simplified model whilst running numerous load scenarios (e.g. SAP2000, Staad-Pro, Robot, etc.). Employing such software is impractical within FE modelling of column base plate and various other connections. The impracticability arises from the softwares' ability to detail surface interactions between steek components and most importantly steel and concrete components. Modelling of base plate connections often requires advanced FE software such as ABAQUS and ANSYS. The software must feature nonlinear complex FE models capable of mimicking all interactions and revealing any possible mechanism. This capability comes at the expense of time requirements and computers capacities. The current research project investigates a headed anchor rod FE model in tension, utilising comprehensive computational analyses on validated FE models (using ABAQUS v.6.10). This leads to the derivation of a simple equation that describes the stiffness of the headed anchor rod embedded in concrete. The thereafter equation could be used in structural software by practicing engineers. Consequently, it enables engineers to analyse base plate connections whilst entering the actual rigidity, rather than assuming fully pinned or fully fixed behaviour. Moreover, this method is not limited to a specific configuration of base plate connections as it can be applied to connections independently of the number of anchor rods and their arrangement.

2. Overview of the experimental work

Extensive experimental works carried out by Petersen et al. [24] studied the behaviour of cast-in-place anchors under monotonic shear, cyclic shear, monotonic tension, cyclic tension, and cyclic combined tension-shear loading. These tests, carried out under monotonic tension, are now used to validate the FE model developed for the purpose of the current study. Each examined block includes four anchors cast in plain concrete. One experimental test, conducted by Petersen et al., was selected to validate the FE model (specimen: 1292010). The edge distance and embedment depth were selected to capture the steel failure. Each anchor was loaded and examined separately. Significant interaction between the cone failures of the first and second anchors tested on the same side of the block, as revealed by Petersen et al. [24].

According to ASTM F1554, 19mm diameter Grade 55 anchor rods were used in the full-scale test with a yield stress, f_y, equal to 434MPa and an ultimate stress, f_u, equal to 524MPa. The width and the length of the plain concrete block are notated in **Fig. 4.** Moreover, two tie-down rods were used during the experimental test to fix the concrete block to the ground floor.

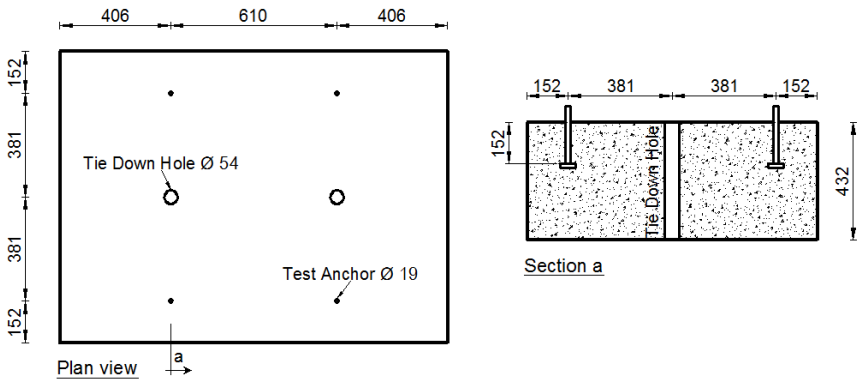

Fig. 4: Geometry of the experimental test

3. Validation of the FE Model

During the experimental tests, each anchor was tested separately. Therefore, only a quarter of the experimental specimen was modelled and analysed. A three-dimensional (3D) FE model with material nonlinearity was created using solid elements.

The geometric characteristics of the FE model (S1) are illustrated in **Fig. 5**. The depth of the experimental concrete block was equal to 432mm; however the depth used in the simulation was reduced to 279mm to limit the computational effort and the corresponding analysis time. A preliminary analysis was performed to ensure that this assumption could be adopted, and reliable results were obtained. The 19mm diameter of the anchor rod was modelled as 17mm to approximate the effect of the threaded section.

The concrete block, the rod and the washer were modelled with 8-node linear brick reduced integration elements (C3D8R). It is worth mentioning that the concrete section away from the anchor assembly was meshed using coarse brick elements while the region that expected to yield is refined with finer elements to obtain accurate results.

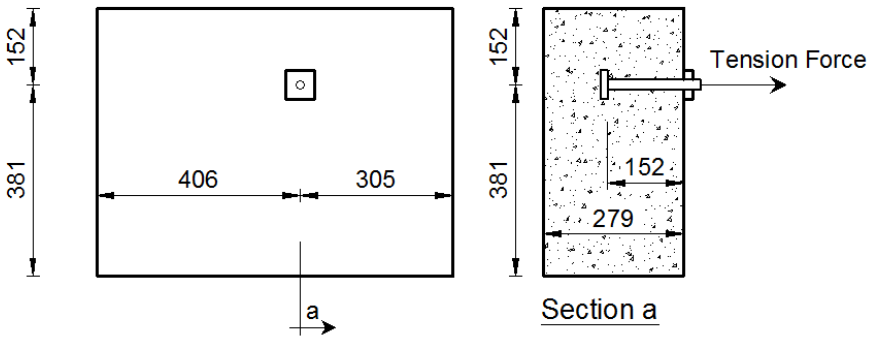

Fig. 5: Geometry of FE models

The bond between the anchor rod and the concrete may fail at an early stage of the load application. It is therefore assumed that from the initiation of loading [3][[16], the tensile force resisted by the anchor plate and the bond can be neglected [23]. As a consequence of this phenomenon and suggestions of previous experimental studies, the anchor rod-concrete bond was ignored during the analysis. This accounts for the mechanism

following the initial failure of the bond, evaluating the force resisted by the bearing between the steel and the concrete. Surface-to-surface contact interaction was assigned between the steel and the concrete components, and a finite sliding formulation selected. The tangential behaviour of the contact interaction was defined as a frictionless formulation.

3.1. Material models

A nonlinear material obeying the Von Mises yield criterion and the isotropic hardening was employed to model the steel components (i.e. anchor and anchor washer). The material properties used are as follows: (i) Young's Modulus, E=218GPa, and (ii) ASTM F1554 Grade 55 anchors with yield stress, f_y=434MPa, and ultimate stress, f_u=524MPa.

The concrete was modelled by applying the damage plasticity approach. Nominal concrete material properties are required to model both the elastic and plastic behaviour in compression and tension, including strain softening and tension stiffening. Therefore, intensive material testing was required (as previously undertaken) to define the parameters required for insertion in the FE software [25]. Within the relevant literature there are a plethora of suggestions discussing the development of concrete behaviour under compression based on experimental tests [26-[29]. The constitutive law for concrete under compression was calculated using an experimentally verified numerical method described by EC2 [30]. This approach was utilised to derive the stress and corresponding strain up to the concrete's nominal ultimate strain, using only the maximum compressive strength. The tension softening curve was developed using Equation 1, as proposed by Hilleborg [31]. The fracture energy of the concrete was taken as equal to 130N/m, and the tensile strength was calculated according to EC2 [30]:

$$\sigma(w) = f_t(1 + 0.5\frac{f_t}{G_f}w)^{-3} \quad (1)$$

where:

σ is the tensile stress, (MPa)

w is the crack opening, (mm)

f_t is the tensile strength, (MPa) and

G_f is the fracture energy of the concrete, (N/mm)

3.2. Boundary and loading conditions

Displacements and rotations of the concrete pedestal were locked at its base. The specimens were monotonically loaded in tension with the displacement control method up to the post-elastic behaviour. Constant displacement was applied at a concentrated reference point tied to the top surface of the anchor rod (**Fig. 6**). However, in the current work the behaviour of the connection within the elastic range is investigated. The load applied during the model validation extended to the failure state, ensuring that the model and the material properties were defined in ABAQUS at a satisfactory level.

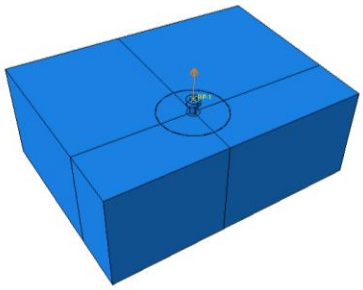

Fig. 6: The application of loading on model

4. Comparison of Experimental against Numerical Results

Fig. 7 compares the tensile force-displacement response of the experimental and the FE models. It is apparent that the FE model correlates successfully with the experimental test during both elastic and plastic stages. The maximum tensile force captured by the FE modelling is equal to the experimental tests (124kN).

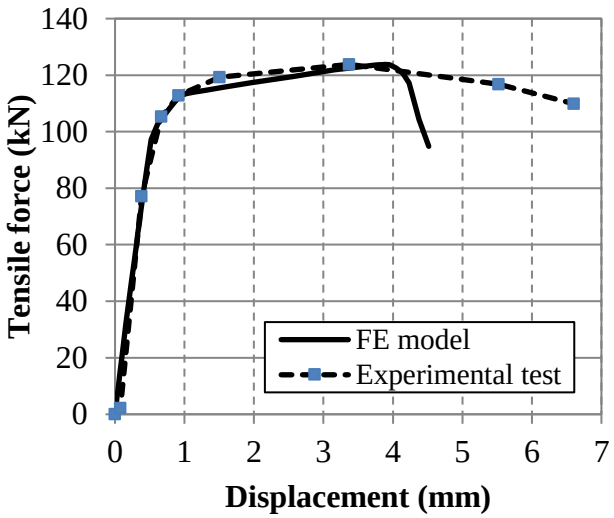

Fig. 7: Comparison of FE model and experimental test results

5. Parametric Studies

An extensive FE study was carried out to investigate the factors that principally affect the strength and the behaviour of anchor rods subject to pure tensile forces. The concrete strength, the embedment depth and the anchor rod diameter are defined as the major factors influencing the behaviour of the anchor rod. The primary variables examined in this project were three. Namely, the embedment depth, the anchor rod diameter, and the anchor plate diameter. It is worth noting that no concrete failure is anticipated. According to the design of such base plates the concrete edge distance provided is suitably significant to prevent concrete failure. Moreover, the presence of reinforcement within the specimens enhances concrete's performance. A series of FE models were developed to investigate the effect of the three aforementioned variables on the capacity of the connection. The diameter and thickness of the anchor plate were kept constant in all models. This enables a study of the connection's strength with respect to changes in

embedment depth or rod diameter. Similarly, the embedment depth was then kept constant to study the effect of the diameter of the anchor plate.

All parametric studies were carried out under pure tensile force in terms of displacement. (The top surface of the anchor was subject to displacement parallel to the axis of the anchor rod.) The applied displacement was increased incrementally during the analysis until the failure of the connection. The element types and the material properties of the anchor rod were the same as those used in the validated model. The cylinder compressive strength of the concrete used in the parametric study was 25MPa.

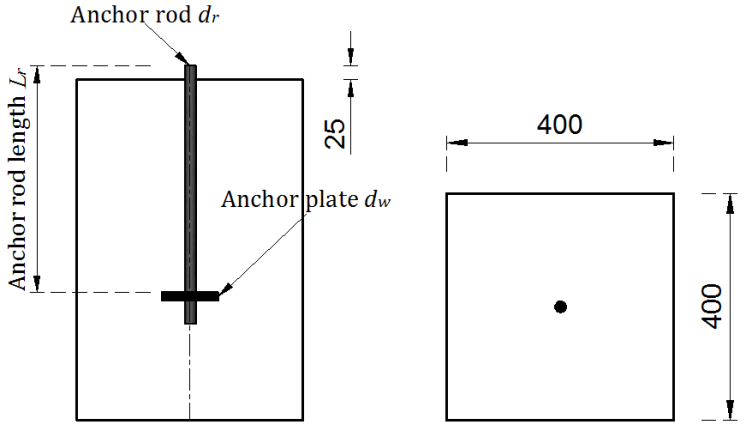

Fig. 8: Geometry of parametric model

Each specimen was represented by a three field identifier as demonstrated in **Fig. 9**. For example D20-L400-W70; is the connection with anchor diameter of 20mm, anchor length of 400mm and diameter of anchor washer plate of 70mm.

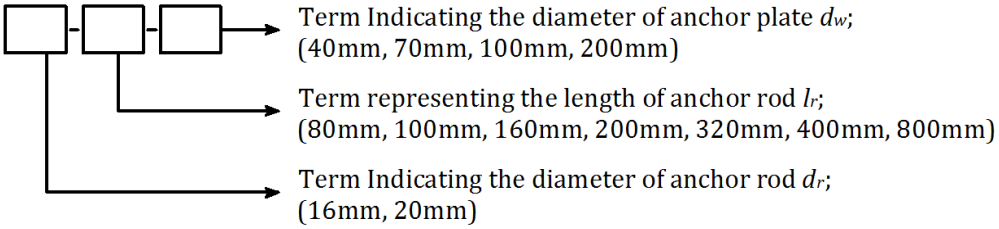

Fig. 9: Specimen Classification

5.1. Influence of the embedment depth

Fig. 10 and **Fig. 11** respectively depict the rod tension force-displacement behaviour of various connections with different embedment depth. It can be observed that embedment depth influenced the stiffness and the elongation of the connection greatly, whilst having a profound effect on the failure mode. It can also be noted that the initial stiffness obtained for the base plate connections was very similar for all models, regardless of the embedment depth. Nevertheless, the final elongation increased significantly with the increase in embedment depth. It was also recorded that the embedment depth did not affect the ultimate tensile strength of the connection. Conversely, in order to avoid the concrete pullout and the cone failure, a minimum embedment depth for concrete cover

was required. The ultimate strength was not affected when the depth used was greater than the minimum cover. For embedment depths greater than $10d_r$, the maximum capacity of the connection was achieved, and the connection failed due to anchor rapture (i.e. no concrete failure occurred).

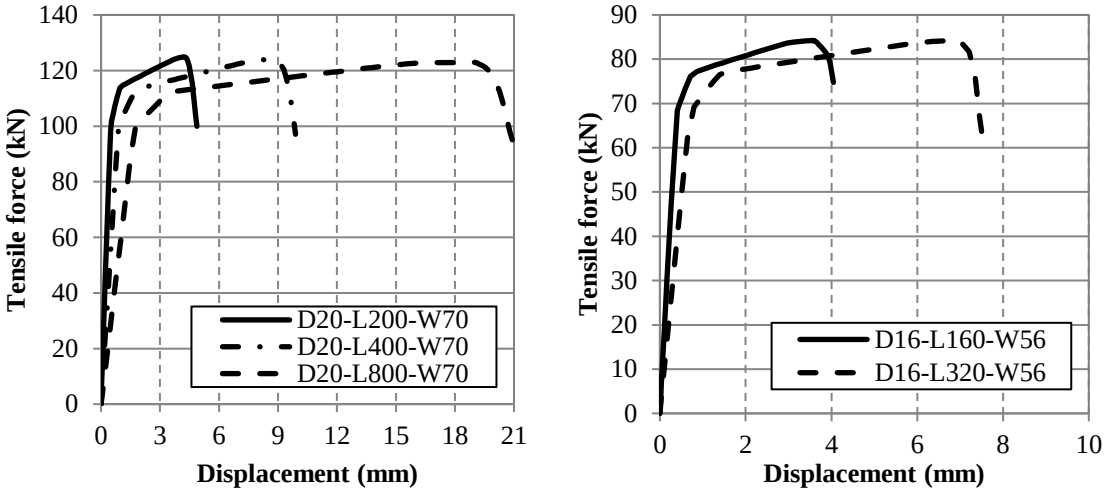

Fig. 10: Force-displacement curve (due to steel failure)

If the concrete above the anchor plate is insufficient to resist the applied load, the crack would extend to the free edge (**Fig. 12**). The concrete cover is rendered unable to resist further loading. **Fig. 11** presents the force-displacement behaviour of FE models failed due to concrete pullout and cone failure. Concrete failure only took place for an embedment depth of $5d_r$. The anchor rod model with a diameter of 20mm reached an ultimate stress at failure loads of approximately 280MPa, 35% lower than its yield strength. An abrupt failure took place for the specimen with embedment depth of $5d_r$; no yielding was observed before the descending curve (**Fig. 11**). This type of failure raises significant risk issues in engineering practice as it gives no warning prior to the collapse. It is therefore advisable to select an embedment depth greater than $10d_r$.

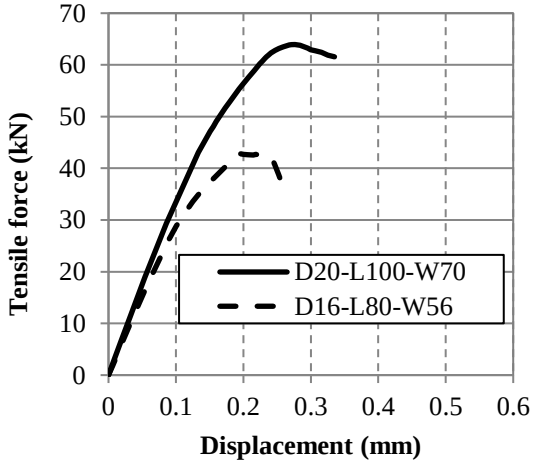

Fig. 11: Force-displacement curve (due to concrete failure)

A typical crack pattern is revealed in **Fig. 12**. It is apparent that the embedment depth of $5d_r$ caused the breakout and pullout failure of the concrete. The angle of the concrete cone failure acquired from the analysis was 35°. This is in line with the value suggested by ACI [2] and CEN/TS [32].

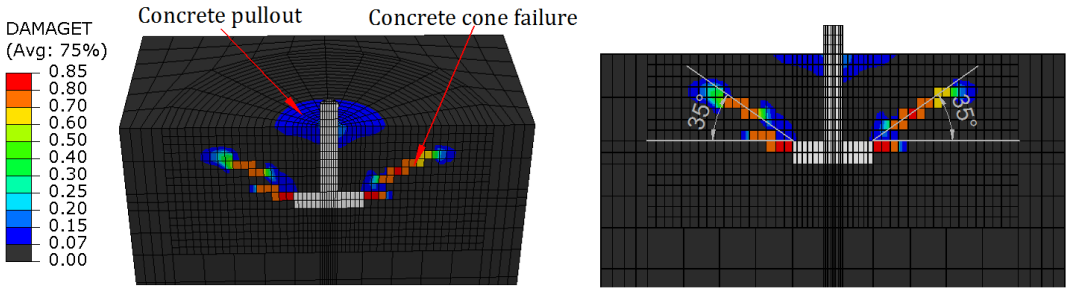

Fig. 12: Concrete cone behaviour using the tensile damage parameter in ABAQUS (D20-L100-W70)

The concrete bearing stress along the depth of the concrete block and in the vicinity of the anchor rod is depicted in **Fig. 13**. Concrete stress was recorded at the onset of the connections' yielding point. (100kN for the anchor rod with diameter of 20mm, and at 70kN for the anchor rod with diameter of 16mm. The elastic limit was not exceeded and the tensile force changed slightly beyond the proportional elastic limit. As it was realised, the maximum bearing stress was reached at the surface of the anchor plate. The stress reduced gradually and completely vanished along the partial depth (i.e. effective depth) of the concrete block. Interestingly, the modelled effective concrete depth was approximately the same when anchors with the same diameter were considered. When equal embedment depths were considered, the effective concrete depth with anchor diameter of 16mm was shallower than those with anchor diameter of 20mm. Thus it is apparent that the depth of the compressive concrete zone correlates with the diameter of the anchor rod at approximately $10d_r$.

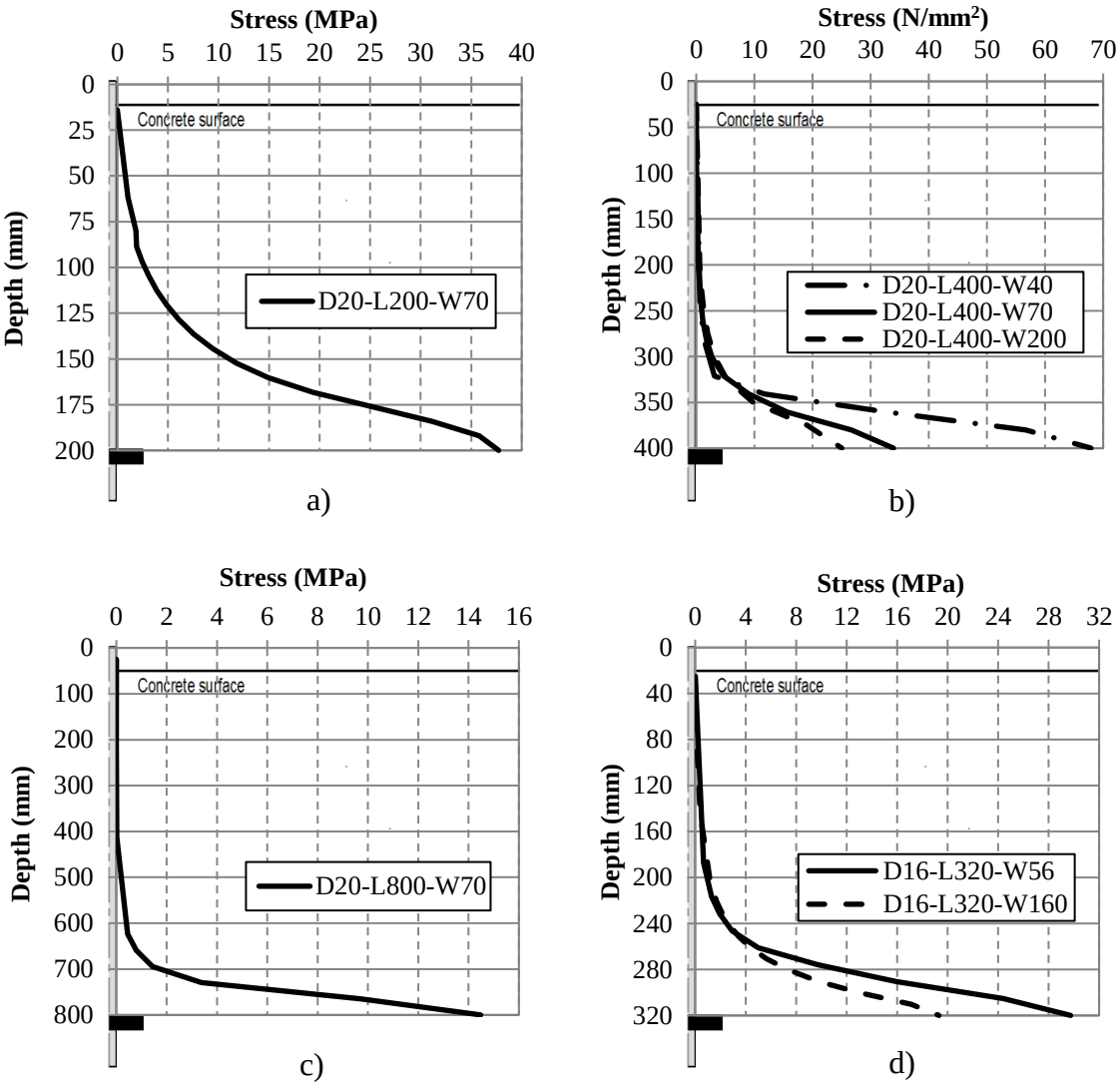

Fig. 13: Concrete bearing stress (measured along the depth near the anchor rod)

5.2. Influence of anchor plate diameter

Three anchor plate diameters ($2d_r$, $3.5d_r$ and $10d_r$) were examined to investigate the effect of the bearing area at the base plate connection. The thickness of the anchor plate was maintained for all specimens, being suitably thick to eliminate the effect of plate bending under applied load. It was observed that the plate diameter did not affect the behaviour of the connection when the anchor rod failure controlled the connection strength. The use of small diameter anchor plates resulted in high-stress concentration in the vicinity of the anchor plate (as shown in **Fig. 13b** and **Fig. 13d**). The stresses acquired from the FE models with a diameter of 20mm and anchor plate rod of 40mm; 70mm and 200mm were 77MPa, 34MPa and 25MPa, respectively. This led, in the case of small anchor plate diameters, to concrete crushing near the plate. It is important to notice that the concrete bearing stress observed in the models with small anchor plate diameters exceeded the ultimate concrete strength. For example, the maximum concrete stress observed in model D20-L400-W40 was 129MPa, approximately five times greater than the concrete strength

(25MPa). It is therefore realised that when confined concrete is considered, high compressive stresses develop under tri-axial stress conditions. Abram [33] observed a concrete bearing stress of 89.64MPa by the concentric pullout specimen featuring an anchor plate at the end of the anchor rod. The cylindrical compressive strength of concrete used in these tests was only 12.8MPa. Hence, the observed concrete bearing stress was seven times higher than the concrete compressive stress.

6. Modelling the Stiffness of the Anchor Rod

Within the design process of column bases, the analytical representation of the structural response of the anchor rod with an anchor plate is of paramount importance. The analytical approach is based on the elastic stress distribution laws. As observed in the parametric study, most of the connection's capacity was achieved within the elastic range. This is in line with the majority of structural design procedures, which do not exceed the elastic limit of the material.

The measured stiffness of the connection, as obtained from load-displacement curves, is considerably less than the stiffness calculated by conventional elastic theory (EA/L). This is attributed to the stiffness calculated by the theoretical approach not taking into account the displacement and the stiffness of the concrete. The proposed process considers the stiffness degradation due to concrete and leads to an equation that defines the stiffness of the anchor rod embedded in concrete.

An anchor rod with diameter, d_r, and length, L_r, subject to tensile force, P, is considered. The total displacement, δ_t, of the rod, is equal to the sum of rod displacement, δ_r, and concrete displacement, δ_c, as described in Equation 2**.**

$$\delta_t = \delta_r + \delta_c \tag{2}$$

The resulting force in the rod and the concrete are similar and equal to the applied force.

$$P_t = P_r = P_c \tag{3}$$

The anchor rod and the concrete can be represented by spring elements with stiffness, K_r and K_c, respectively. Since the total displacement is equal to the sum of the rod and the concrete displacement, the two springs are in series as demonstrated in **Fig. 14**, and the total stiffness K_t can be derived as following:

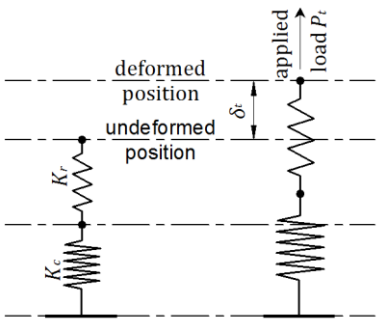

Fig. 14: Mass-spring model of the anchor rod under pure tensile force

$$\frac{P_t}{K_t} = \frac{P_r}{K_r} + \frac{P_c}{K_c} \tag{4}$$

As stated in **Equation 2**, both concrete and anchor rod forces are the same and equal to the applied force, hence:

$$\frac{1}{K_t} = \frac{1}{K_r} + \frac{1}{K_c} \tag{5}$$

Rearranging the equation gives:

$$K_t = \frac{K_r \bullet K_c}{K_r + K_c} \tag{6}$$

and from the basic equations of mechanics of material:

$$E = \frac{\sigma}{\varepsilon} = \left(\frac{P}{\delta}\right)\left(\frac{L}{A}\right) = K\frac{L}{A} \tag{7}$$

and then:

$$K_r = \frac{E_s \bullet A_r}{L_r} \tag{8}$$

and:

$$K_c = \frac{E_c \bullet A_c}{L_c} \tag{9}$$

where:
E_c and E_s are Young's Modulus for concrete and steel, respectively, and L_c and A_c are the stressed lengths and stressed area of the concrete, respectively, as depicted in **Fig. 15**.

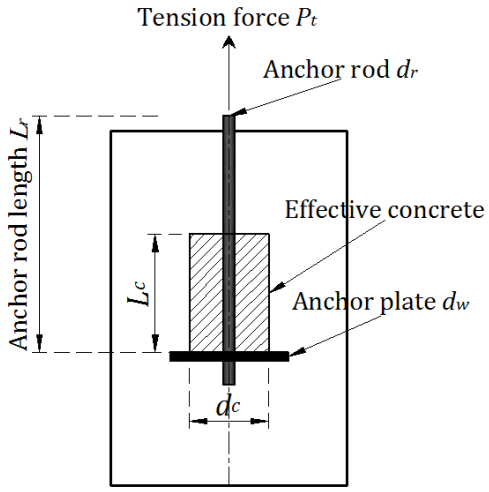

Fig. 15: Effective concrete

Substituting Equation 8 and 9 into 6 gives:

$$K_t = \frac{E_s A_r \bullet E_c A_c}{E_s A_r L_c + E_c A_c L_r} \tag{10}$$

Dividing Equation 10 by E_c gives:

$$K_t = \frac{E_s A_r \bullet A_c}{n A_r L_c + A_c L_r} \tag{11}$$

where: $n = \frac{E_s}{E_c}$

It was observed from the parametric analysis that the maximum stress is found near the anchor rod, while the stress distribution over the anchor plate was linear, as illustrated in **Fig. 16**. The diameter of the effective concrete area was approximately $3.5d_r$. In addition, it was concluded that the depth of the effective concrete was approximately ten times the diameter of the anchor rod, hence:

$$K_t = \frac{E_s A_r}{0.8 n d_r + L_r} \tag{12}$$

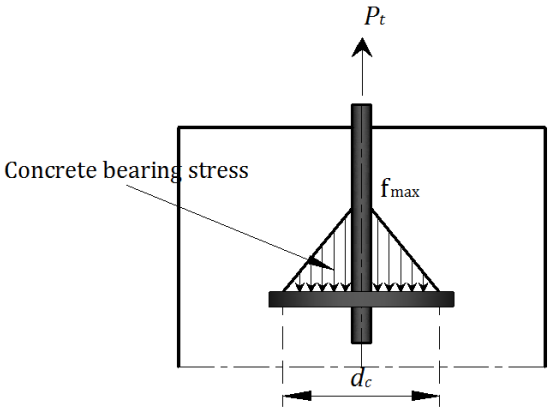

Fig. 16: Stress distribution in concrete in the vicinity of the anchor rod

Table 1 compares the stiffness obtained from the FE analyses and the stiffness calculated by Equation 12. It is proved that the proposed equation predicts the stiffness of the anchor rod embedded in concrete accurately.

Table 1: Comparison of stiffness

Test Notation	d_r *(mm)*	Concrete		Stiffness (N/mm)		$\frac{K_{Abaqus}}{K_{Eq.12}}$
		E_c *(GPa)*	f_{cm} *(MPa)*	K_{Abaqus}	$K_{Eq.12}$	
D20-L100-W70	20	29	25	309800	305628	1.02
D20-L200-W70	20	29	25	201000	208868	0.97
		32	40	205510		0.99
D20-L400-W70	20	29	25	115000	127890	0.9
		32	40	115750		0.91
D20-L800-W70	20	29	25	59500	72035	0.83
D16-L80-W56	16	29	25	248700	244503	1.02
D16-L160-W56	16	29	25	183300	167095	1.1
D16-L320-W56	16	29	25	96650	102312	0.95
D20-L400-W100	20	29	25	114470	127890	0.9
D20-L400-W200	20	29	25	113600	127890	0.89
D16-L320-W160	16	29	25	96900	102312	0.95
		32	40	97560		0.96
D20-L400-W40	20	29	25	110000	127890	0.87

7. Verification and Applications of Derivative Equation

The stiffness, as estimated by Equation 12, can be used as an input to the available structural analysis software (such as SAP2000) using a spring coefficient to simplify the modelling of the base plate connections. To verify the SAP2000 model and illustrate the use of the derived equation, three different configurations of base plate connections were modelled. ABAQUS and SAP2000 software was used, and the results were compared.

The tension developed in the anchor rods, the angle of rotation of the base plate, and the resulting stress in the base plate were the main characteristics compared.

The first model F1 (**Fig. 17**) was selected from the experimental campaign carried out and presented by Gomez et al. [34] (test #M1 in phase II). This particular type of base plate connection has undergone extensive studies [16][[18-[21] [[35]. It was thus identified and used to validate the proposed equation and the FE model. It was examined under uniaxial moment whilst the compressive force was not applied.

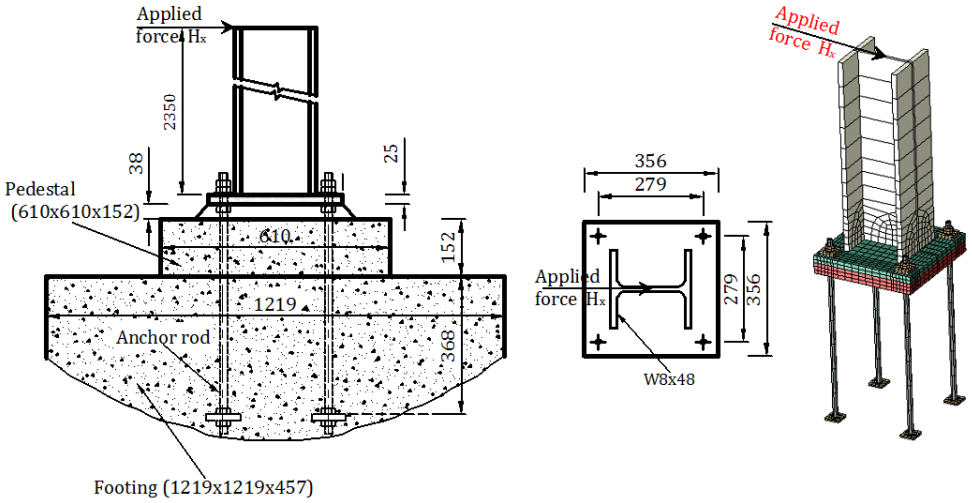

Fig. 17: Geometry of model F1

A more intricate arrangement of anchor rods and loading, was considered in models F2 and F3. Both models were examined under biaxial moment and compressive force. These types of connections were not previously considered by researchers as it was deemed complicated to apply the component method to such configurations. **Fig. 18** and **Fig. 19** illustrate the dimensions of model F1 and F2, respectively.

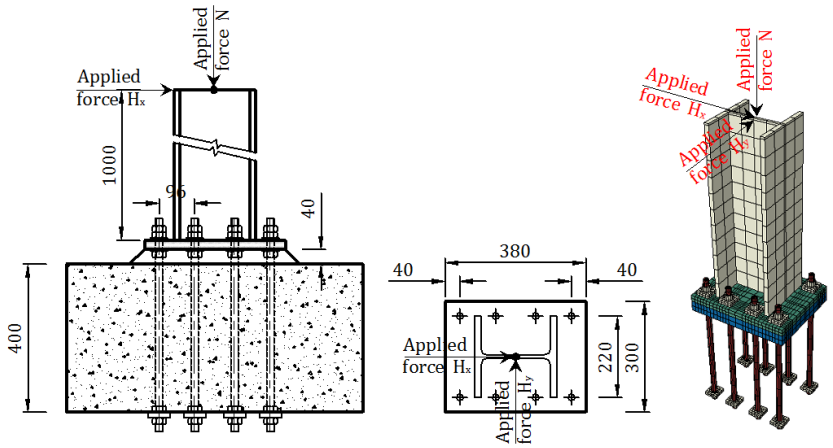

Fig. 18: Geometry of model F2

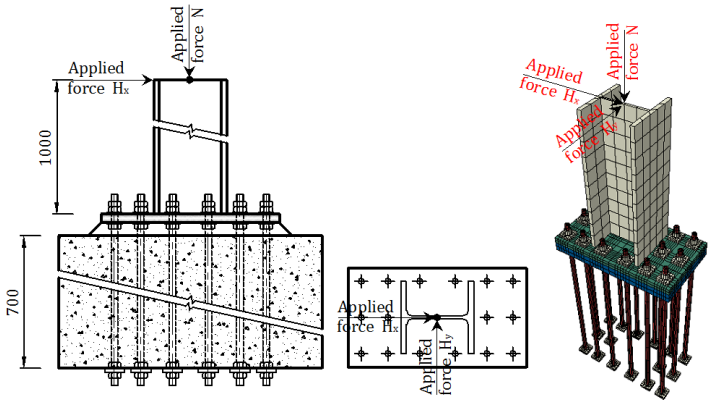

Fig. 19: Geometry of model F3

7.1. SAP2000 modelling

SAP2000 v.15 was used in this study as it is widely used in engineering practice. The aim of employing the three-dimensional models and analysis conducted by SAP2000 is to enable structural design engineers to visualise the forces/stresses developed in the anchor rods and the base plates in complex column base connection configurations. The FE models are examined under shear force, axial force and bending moments to represent the majority of loading scenarios occurring in real situations.

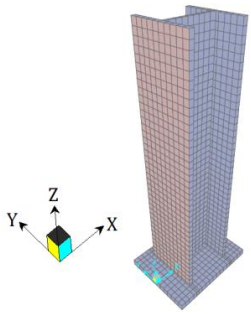

Fig. 20: Extrude view of SAP2000 model

Shell elements were used to simulate the structural components of the connections. The columns and the base plates are modelled using those elements as shown in **Fig. 20**. The column height used in the analysis was measured from the centreline of the base plate to the top of the column. Each component of the column base connections was defined with appropriate shell thickness. For example, in model F2 and F3, the shell thickness of the column flange and web are defined equal to the flange and web thickness of HEB220 (i.e. 16mm and 9.5mm).

Three types of boundary conditions were applied to the SAP2000 models. Tension springs were utilised to represent the anchor rods. Their stiffness was calculated using Equation 12 before being assigned to the software at the location of the anchor rods in the Z direction. Shear force was assumed to be carried by the anchor rods. The directions of the shear actions (i.e., in X and Y directions) were fully restrained at the location of the anchor rods. The concrete was simulated by compression springs, as it does not carry any tension forces. The spring stiffness assigned to SAP2000 was calculated based on

ABAQUS analysis output. The ABAQUS bearing stress for concrete was divided by the vertical deflection at that point. Numerous points were examined along the concrete stiffness calculation, with the value of concrete stiffness ranging between 120N/mm/mm^2 and 170N/mm/mm^2. SAP2000 model was examined using both stiffness magnitudes while it was observed that their effect was negligible. The average stiffness magnitude of 145N/mm/mm^2 was thus considered in this study. **Fig. 21** represents the springs assigned to the anchor rods and the base plate. Only compression springs were considered when defining the area of the spring at the bottom face of the shell elements of the base plate.

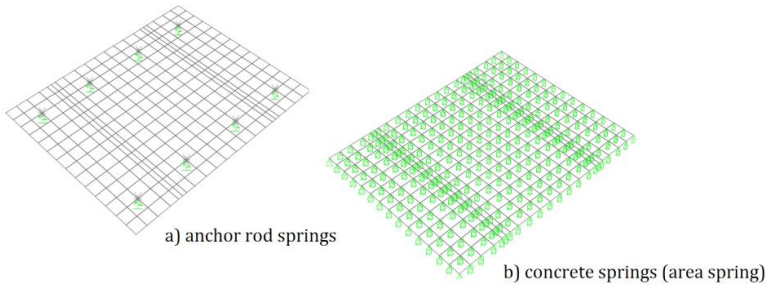

Fig. 21: Spring locations

7.2. Comparison of anchor rod force

Fig. 22 shows the comparison of anchor tension force between SAP2000 and ABAQUS software for all models. It is apparent that the anchor force obtained from SAP2000 models was remarkably similar to the force captured from the ABAQUS analysis. Furthermore, for model F1 the tension force developed in anchor rods during the analysis and the experimental tests carried out by Gomez [34] was approximately identical. Similarly, in more complicated configurations and loadings the proposed equation in line with SAP2000 still yields remarkable results as the difference between the forces in the critical anchor does not exceed 2%.

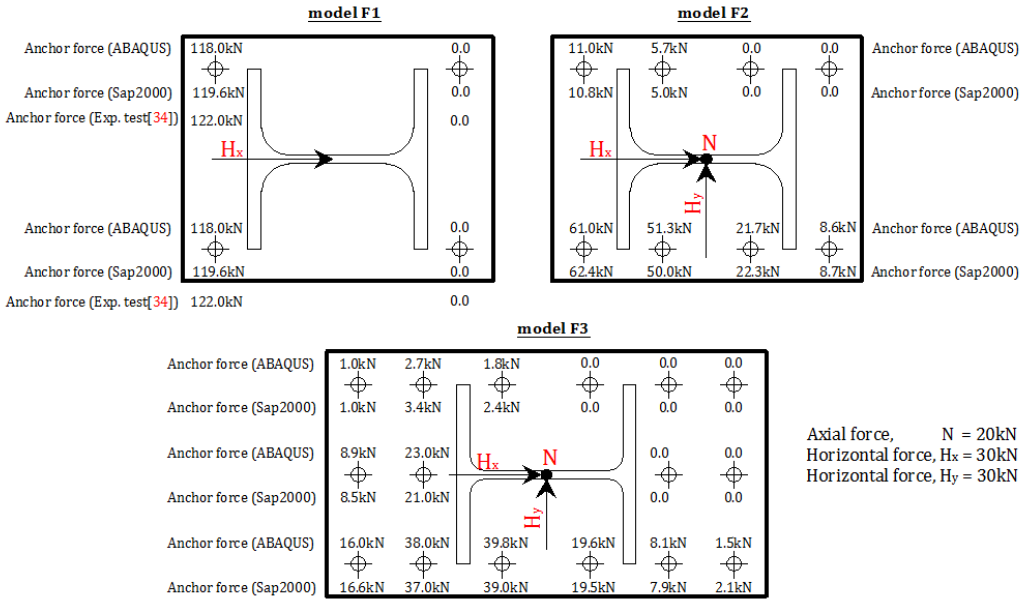

Fig. 22: Comparison of tension in anchor rods

7.3. Comparison of rotation of base plate

Table 2 provides a comparison of the base plate rotation for both major and minor directions. The angle of rotation was calculated by dividing the lateral drift at the top of the column by the height of the column in each direction separately. It is apparent that the SAP2000 model yields slightly lower values than the one obtained using ABAQUS, (ranging between 7% and 3%).

Table 2: Comparison of base plate rotation

Model	Base plate rotation in major direction ($\varphi_x \times 10^{-3}$)			Base plate rotation in minor direction ($\varphi_y \times 10^{-3}$)	
	Exp. Test [34]	ABAQUS	SAP2000	ABAQUS	SAP2000
F1	14.56	14.53	13.6	N.A	N.A
F2	N.A	2.63	2.53	3.82	3.62
F3	N.A	2.38	2.32	4.1	3.93

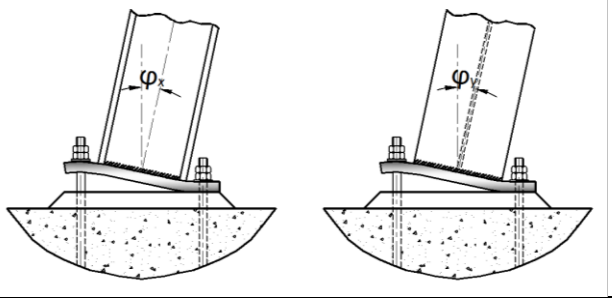

7.4. Comparison of base plate stress

Fig. 23 to **Fig. 25** demonstrate the comparison of the stresses in the base plates obtained by ABAQUS and SAP2000 software, respectively. It is undoubtedly observed that the stress pattern is very similar for both models with SAP2000 models producing higher stress magnitudes at the points of force concentration. In the vicinity of such stressed areas, SAP2000 presents higher numbers than ABAQUS by 20% to 40%. However, it is worth noting that similar stress magnitudes were observed in the non-highly stressed zones.

The reason for the deviation of the results between SAP2000 and ABAQUS models is due to the following issues:

- The base plate boundary conditions in SAP2000 models is applied at nodes while in ABAQUS there was a contact surface (e.g. base-grout). This might cause a force concentration at nodes where boundary conditions were applied which then produces high-stress concentrations.

- It is considered that the mesh elements used in SAP2000 might result in high-stress concentrations. The washer supports the base plate in the vertical direction, thus, the tension is developed in the anchor rods. The surface of the washer provides some stress distribution on the base plate. In contrast, no washer was modelled in SAP2000, and the tension developed in the anchor rod was

concentrated at one point. Conversely, in ABAQUS the steel column transfers its load onto the contact surface of the base plate and the column while in SAP2000 it distributes the load on a line.

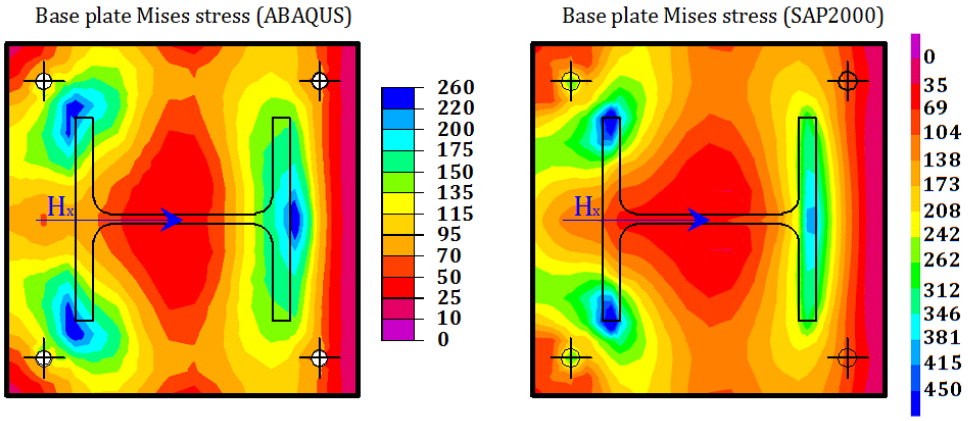

Fig. 23: Comparison of base plate stress (F1)

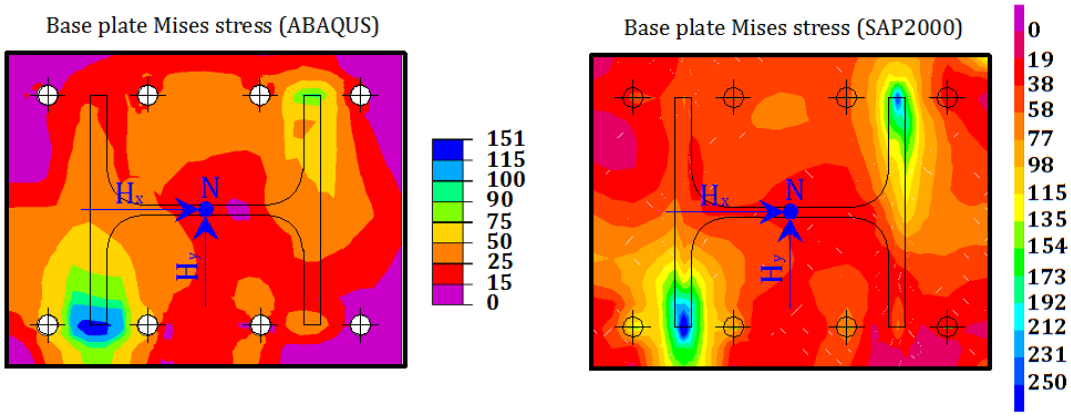

Fig. 24: Comparison of base plate stress (F2)

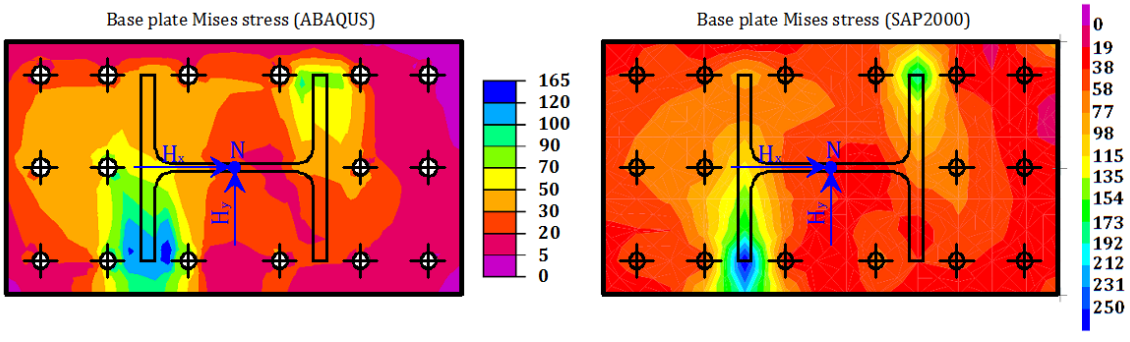

Fig. 25: Comparison of base plate stress (F3)

8. Conclusion

From the review of previous studies, it appears that primarily standard configurations of column base plate connections with two or four anchor rods were considered. Alterntively, connections with higher numbers of anchor rods or complicated scenarios of applied force are rather scanty. This paper proposed to analyse and design column base connections regardless of complicated arrangements of anchor rods and the magnitude of the applied forces. The proposed solution was preceded by a parametric study to investigate the factors affecting the behaviour and strength of a headed anchor rod in tension using a three-dimensional model in ABAQUS v6.10. The following conclusions have been drawn.

- The embedment depth has a profound effect on the final elongation of the anchor rod and affects the failure mode. Moreover, it was observed that the initial stiffness and the strength of the connection were independent of the embedment depth when the anchor rod rapture controls the connection strength.

- The diameter of the anchor plate does not affect the behaviour and strength of the connection. Nevertheless, a high-stress concentration in the vicinity of the anchor plate is expected when the small diameter plate is used.

- The proposed mathematical equation proves that headed anchor bolts can be represented by mass-spring models taking into account the stiffness of the rod and the concrete. The stiffness obtained by the proposed analytical formula with corresponding FE results is satisfactory.

- The stiffness calculated by the proposed equation can be used as input to the available structural software (such as SAP2000) using a spring coefficient to simplify the modelling of the base plate connections. The simplified model gives remarkable results for tension developed in the anchor rods and angle of rotation of the base plate. However, as a resutl of certain factors (eg. stress concentration and boundary condition in SAP2000 models), base plate stress is higher than expected in the vicinity of stress concentrations, while similar stress magnitudes were observed in the low stress zones.

References

[1] Akiyama, H. (1985) “Seismic Design of Steel Column for Architecture.” in Japanese, Gibodoskupan, Tokyo 1985.
[2] ACI Committee 318. (2008) “Building Code Requirements for Structural Concrete (ACI 318-02) and Commentary (ACI 318R-02),” Farmington Hills, MI.
[3] Delhomme, F., Debicki, G. and Z. Chaib. (2010) “Experimental behaviour of anchor bolts under pullout and relaxation tests” Construction and Building Materials Vol. 24, No 3, pp. 266–274.

[4] Hasselwander, G.B., Jirsa, J.O., Breen, J.E. and Lo, K. (1977) “strength and behaviour of anchor bolts embedded near edges of concrete piers.” Final Report Texas Univ., Austin. Center for Highway Research.
[5] Gomez, I.R., Kanvinde, A.M., Smith, C., and Deierlein, G.G. (2009) “Shear Transfer in Exposed Column Base Plates,” Technical Report submitted to the American Institute of Steel Construction, AISC, Chicago, Illinois.
[6] DeWolf, J.T. and Ricker, D.T. (2003) “Column Base Plates,” 3rd Ed., Steel Design Guide Series No. 1, American Institute of Steel Construction, Inc., Chicago, IL.
[7] Fisher, J.M. and Kloiber, L.A. (2006) “Base Plate and Anchor Rod Design,” 2nd Ed., Steel Design Guide Series No. 1, American Institute of Steel Construction, Inc.,Chicago, IL.
[8] ACI 349-79. (1976) Code requirements for nuclear safety related concrete structures. Detroit: American Concrete Institute, 1976.
[9] Eurocode 3. (2005) Design of steel structure – Part 1–8: design of joints. Brussels: European Standards, CEN, 2005.
[10] Ashour, A.F. and Alqedra, M.A. (2004) “Concrete breakout strength of single anchors in tension using neural networks,” Advances in Engineering Software 36 (2005) 87–97.
[11] Eligehausen, R., Fuchs, W. and Sippelt T.M. (2004) “Anchorage to concrete,” Progress in Structural Engineering and Materials Vol. 1, Issue 4, pp 392–403.
[12] ACI Committee 355. (1997) “State-of-the-art report on anchorage to concrete,” Detroit, USA: American Concrete Institute; 1991. Reapproved 1997.
[13] Comite Euro-International du Beton (CEB), (1994) Task Group VI/5. “Fastenings to concrete and masonry structures,” London, UK: Thomas Telford Services Ltd; 1994. p.p.249.
[14] Fuchs, W., Eligehausen, R. and Breen, J.E. (1995) “Concrete capacity design (CCD) approach for fastening to concrete,” ACI Struct J 1995;92(1):73–94.
[15] Cook, R.A., Collins, D.M., Klingner, R.E. and Polyzois D. (1992) “Load-deflection behavior of cast-in-place and retrofit concrete anchors,” ACI Struct J 1992;89(6):639–49.
[16] Jaspart, J.P. and Vandegans, D. (1998) “Application of Component Method to Column Bases,” Journal of Constructional Steel Research, Vol. 48, pp. 89-106.
[17] Wald, F., Sokil, Z. and Jaspart, J.P. (2008) "Base plate in bending and anchor bolts in tension." Heron 53.1/2.
[18] Kontoleon, M.J., Mistakidis, E.S., Baniotopoulos, C.C. and Panagiotopoulos, P.D. (1999) "Parametric analysis of the structural response of steel base plate connections." Computers & Structures 71, no. 1: 87-103.
[19] Baniotopoulos, C.C., Sokol, Z. and Wald, F. (1999) "Column base connections." COST CI Report of WG6-Numerical simulation. Brussels-Luxemburg: European Commission, pp. 32-47.
[20] Ermopoulos, J.C. and Stamatopoulos, G.N. (1996) "Mathematical modelling of column base plate connections." Journal of Constructional Steel Research 36, no. 2, pp. 79-100.
[21] Stamatopoulos, G.N. and Ermopoulos, J.C. (2011) "Experimental and analytical investigation of steel column bases." Journal of constructional steel research 67, no. 9, pp. 1341-1357.

[22] Melchers, R.E. (1992) "Column-base response under applied moment." Journal of Constructional Steel Research 23, no. 1, pp. 127-143.
[23] Stark, J., and Hordijk, D.A. (2001) "Where structural steel and concrete meet." Connections between steel and concrete, University of Stuttgart, ed. Eligehausen R., Stuttgart, pp. 1-11.
[24] Petersen, D., Lin Z. and Zhao J. (2013), "Behavior and Design of Cast-in-Place Anchors under Simulated Seismic Loading," Technical Report Submitted to National Science Foundation for the NEESR Project Funded under Grant No. CMMI-990712342.
[25] Wahalathantri, B.L., Thambiratnam, D.P., Chan, T.H.T., and Fawzia, S. (2011) "A Material model for flexural crack simulation in reinforced concrete elements using abaqus" eddBE2011 Proceedings pp. 260-264.
[26] Tsavdaridis, K.D., D'Mello, C. and Huo, B.Y. (2013) "Experimental and computational study of the vertical shear behaviour of partially encased perforated steel beams". Engineering Structures, 56, pp. 805–822.
[27] Tsavdaridis, K.D., D'Mello, C. and Huo, B.Y. (2009) "Shear Capacity of Perforated Concrete-Steel Ultra Shallow Floor Beams (USFB)". Paper presented at the 6th National Concrete Conference, TEE, ETEK, 21-–23 Oct. 2009, Paphos, Cyprus.
[28] Hsu, L.S. and Hsu, C.T.T. (1994) Complete stress-strain behaviour of high-strength concrete under compression. Magazine of Concrete Research, 46(169), pp. 301-312.
[29] Samani, A.K., Attard, M.M. (2012) "A stress–strain model for uniaxial and confined concrete under compression". Engineering Structures, 41, pp. 335–349.
[30] British Standards Institution. (2004) Eurocode 2: Design of Concrete Structures: Part 1-1: General Rules and Rules for Buildings. British Standards Institution, 2004.
[31] Hilleborg, A. (1989) "Stability problems in fracture mechanics testing", Fracture of concrete and rock edited by Shah, S. P., Swartz, S. E. and Barr, B., Elsevier Applied Science, pp. 369-378.
[32] CEN/TS 1992-4-2: Design of fastenings for use in concrete - Part 4-2: Headed Fasteners. 2009. Brussels.
[33] Abrams, D.A. (1913) "Test of Bond between Concrete and Steel," University of Illinois Bulletin, No.71.
[34] Gomez, I., Kanvinde, A.M. and Deierlein, G.G. (2010) "Exposed column base connections subjected to axial compression and flexure." Report Submitted to the American Institute of Steel Construction (AISC), Chicago, IL.
[35] Ermopoulos, J.C. and Stamatopoulos, G.N. (1996) "Analytical modelling of column-base plates under cyclic loading." Journal of constructional steel research 40, no. 3, pp. 225-238.